DOI: 10.1002/chem.201900281

π-Conjugated Polymers

A π-Conjugated, Covalent Phosphinine Framework

Jieyang Huang,[a, b] Ján Tarábek,[b] Ranjit Kulkarni,[a, b] Cui Wang,[c, f] Martin Dračínský,[b] Glen J. Smales,[d] Yu Tian,[e] Shijie Ren,[e] Brian R. Pauw,[d] Ute Resch-Genger,[c] and Michael J. Bojdys*[a, b]

Abstract: Structural modularity of polymer frameworks is a key advantage of covalent organic polymers, however, only C, N, O, Si, and S have found their way into their building blocks so far. Here, the toolbox available to polymer and materials chemists is expanded by one additional nonmetal, phosphorus. Starting with a building block that contains a λ^5-phosphinine (C_5P) moiety, a number of polymerization protocols are evaluated, finally obtaining a π-conjugated, covalent phosphinine-based framework (CPF-1) through Suzuki–Miyaura coupling. CPF-1 is a weakly porous polymer glass (72.4 $m^2 g^{-1}$ BET at 77 K) with green fluorescence ($\lambda_{max} = 546$ nm) and extremely high thermal stability. The polymer catalyzes hydrogen evolution from water under UV and visible light irradiation without the need for additional co-catalyst at a rate of 33.3 $\mu mol\, h^{-1} g^{-1}$. These results demonstrate for the first time the incorporation of the phosphinine motif into a complex polymer framework. Phosphinine-based frameworks show promising electronic and optical properties, which might spark future interest in their applications in light-emitting devices and heterogeneous catalysis.

Introduction

The unique selling point of covalently linked organic materials—according to the claims of polymer and materials chemists—is their LEGO™-like design. That means that there is hypothetically an infinite number of organic building blocks (tectons) at our disposal for their fabrication. However, in reality, only a small subset of all available nonmetals has been incorporated into complex polymers, chiefly aromatic carbon. Such materials as porous organic frameworks (POFs),[1] conjugated microporous polymers (CMPs),[2] and porous aromatic frameworks (PAFs)[3] have been extensively investigated in the fields of gas and energy storage,[4] catalysis,[5] sensing,[6] and in various opto-electronic devices.[7] Incorporation of heteroatoms such as nitrogen, sulfur, and silicon into the backbone of these polymers yields triazine-based graphitic carbon nitride (TGCN),[8] covalent triazine-based frameworks (CTFs),[9] sulfur- and nitrogen-containing porous polymers (SNPs),[10] and silicate organic frameworks (SiCOFs).[11] This has not only led to recent breakthroughs in our understanding of how to construct such extended systems, but it has also uncovered new layers of complexity in material properties. For example, nitrogen-containing CTFs can be used as heterogeneous Periana catalysts and enable low-temperature oxidation of methane to methanol.[12] Further, sulfur- and nitrogen-containing polymers feature intimately linked donor–acceptor domains and a narrow band gap, which result in record-breaking performances in photocatalytic water splitting.[13] Despite the confusing three-letter nomenclature in this field, CTFs, CMPs, PAFs, and SNPs have chiefly in common that they are constructed from covalently linked π-conjugated building blocks;[1–3,9–10] electron delocalization in the polymer framework can improve their intriguing properties, especially electric storage and conductivity, band gap properties, photoluminescence, and light harvesting.[14] Strategies to expand the properties and applications of π-conjugated frameworks can be broadly divided into two categories; post-synthetic modifications and initial reaction

[a] Dr. J. Huang, R. Kulkarni, Dr. M. J. Bojdys
Department of Chemistry, Humboldt-Universität zu Berlin
Brook-Taylor-Str. 2, 12489 Berlin (Germany)
E-mail: m.j.bojdys.02@cantab.net

[b] Dr. J. Huang, Dr. J. Tarábek, R. Kulkarni, Dr. M. Dračínský, Dr. M. J. Bojdys
Institute of Organic Chemistry and Biochemistry of the CAS
Flemingovo nám. 2, 166 10 Prague (Czech Republic)

[c] C. Wang, Dr. U. Resch-Genger
Division Biophotonics
Federal Institute for Materials Research and Testing (BAM)
Richard- Willstätter-Straße 11, 12489 Berlin (Germany)

[d] Dr. G. J. Smales, Dr. B. R. Pauw
Bundesanstalt für Materialforschung und -prüfung (BAM)
Unter den Eichen 87, 12205 Berlin (Germany)

[e] Y. Tian, Dr. S. Ren
College of Polymer Science and Engineering
State Key Laboratory of Polymer Materials Engineering
Sichuan University, Chengdu 610065 (P. R. China)

[f] C. Wang
Institute of Chemistry and Biochemistry
Free University of Berlin, Takustrasse 3
14195 Berlin (Germany)

Supporting information and the ORCID identification number(s) for the author(s) of this article can be found under: https://doi.org/10.1002/chem.201900281.

design. Post-synthetic modifications rely on a number of tools such as changes of the polymer topology (e.g., by template removal, freeze-drying),[15] or various reactions that introduce heteroatoms into the backbone of the network.[16] Although post-synthetic modifications enable interesting enhancements of material properties, they are all strongly dependent on initial framework morphologies (compact or open) and suffer from randomness and inhomogeneity in the case of diffusion-limited processes. Hence, a more rational pathway to improved π-conjugated frameworks is the initial design of building blocks ("tectons").[1–2,7,14,17] Design of tectons is the most exciting and promising field for further exploration, as hitherto only tectons containing the nonmetals C, N, O, and S have been explored in any depth.[9–10,18]

All main-group elements in the first three rows of the periodic table with four to six valence electrons can form aromatic rings. Lower stability may be the reason why Si and P, which are light elements in the third period of the periodic table and in the same groups as C and N, have never been introduced into π-conjugated frameworks.[19] Phosphorus is an outstanding candidate atom to be incorporated into the backbone of materials for a number of reasons: (1) P is electron rich with five valence electrons, like its group V neighbor nitrogen, although it has a larger atomic radius with weaker electronegativity;[20] (2) the polarity of the C–P bond makes P partially positively charged;[20b] (3) phosphorus has a wide range of bonding environments, valence states, and coordination numbers to achieve more probable spatial configurations of repeating units;[20a,21] (4) P can increase the thermal stability of polymers.[22] Moreover, phosphorous-containing molecules are interesting homogeneous catalysts and luminescent dyes.[23]

A variety of P-containing polymer frameworks or graphitic materials have been prepared and applied in water treatment, halogen-free flame retardants, transition metal-catalysis, photocatalysis, lithium batteries, gas-selective membranes, and in the biomedical field.[24] However, none of these P-containing materials is rationally designed or incorporates phosphorous in an overall aromatic, stable network.[25] For example, the P-doped graphitic materials obtained in the past have an entirely random distribution of phosphorus sites.[20b,26] Although the effects of P-doping are real, such statistical functionalizations make it inherently difficult to rationalize any of the observed phenomena.

For the rational design of a π-conjugated, P-containing network, we chose phosphinine—a C_5P ring, equivalent to pyridine—as the principle building block.[19b] Since phosphinine was first synthesized by Märkl in 1966,[27] derivatives of these six-membered C_5P rings have been studied and analyzed for decades. Phosphinines can contain λ^3-phosphinine (a trivalent phosphorus atom with a coordination number of 2) and λ^5-phosphinine (a pentavalent phosphorus atom with a coordination number of 4). They show superior fluorescent properties and have applications in organophosphorus chemistry, coordination chemistry, optoelectronics, and homogeneous catalysis.[19b,25a,28] Although a multitude of molecular reactions and their mechanisms are known, to this day, not one polymer based on phosphinines has been achieved.[25a,29] We believe this is because of the high relative reactivity of the phosphinine P-atom, which renders phosphinine incompatible with most polymerization protocols. For λ^3-phosphinine, the typical electrophilic attack or nucleophilic attack is more preferred at the P atom.[30] λ^5-Phosphinine is more stable owing to the absence of phosphorus lone pairs, but some strong acids or bases can still attack the P atom during some polymerizations.[25a] Therefore, stable phosphinine-based monomers and mild polymerization routes need to be carefully chosen to achieve P-containing π-conjugated frameworks.

In this work, we synthesize a stable λ^5-phosphinine-based tecton, and evaluate its stability in a series of common polymerization protocols. We identify Pd-catalyzed Suzuki–Miyaura coupling as the best approach and, thus, obtain the first P-containing fully aromatic covalent phosphinine-based framework (CPF-1). The structure and properties of CPF-1 were analyzed in detail with a particular focus on optical and electronic factors, which are unique to the high content of aromatic phosphorus in the structure.

Results and Discussion

Design of phosphinine-based monomers

We designed phosphinine-based building blocks with C_{2v} symmetric bonding axes to achieve fully crosslinked frameworks in analogy to triazine-based frameworks (CTFs).[9,31] As the phosphinine P atom influences the reactivity of directly attached substituents considerably,[29c] we chose to include aryl spacers on which the polymerizable reactive groups are situated. Combining several reports about synthesis of aryl halide-substituted λ^3-phoshpinines,[32] and the bromophenyl coupling reaction,[33] we obtain 2,4,6-tri(4-bromophenyl)-λ^3-phosphinine (**3**) as the principle P-containing tecton. As previous reports suggest a high reactivity (and hence low stability) of λ^3-phosphinine, we further synthesize the corresponding, protected λ^5-phosphinine compound, 1,1-dimethoxy-2,4,6-tri(4-bromophenyl)-λ^5-phosphinine (**4**) as another P-containing tecton.[25a] The synthetic routes to monomer **3** and monomer **4** and the subsequent, successful polymerization of tecton **4** to CPF-1 are described in detail in Figure 1.

Stability of phosphinine-based monomers under common polymerization protocols

We have investigated several conventional, mild polymerization protocols to achieve phosphinine-based polymer networks, via reactions of bromophenyl, or its derivative groups of ethynylphenyl and benzonitrile, as shown in Table S1 (in the Supporting Information).[9b,34] As λ^3-phosphinine in particular is very reactive, we evaluated whether the solvent or catalyst attacks the ring-phosphorus during the polymerization reaction. After setting up the polymerization of **3** or **4** under conditions described in Table S1 (in the Supporting Information), the stability of the phosphinine moiety was checked periodically by ^{31}P NMR spectroscopy. The stabilities of the phosphinine moieties **3** and **4** under different reaction conditions are listed in

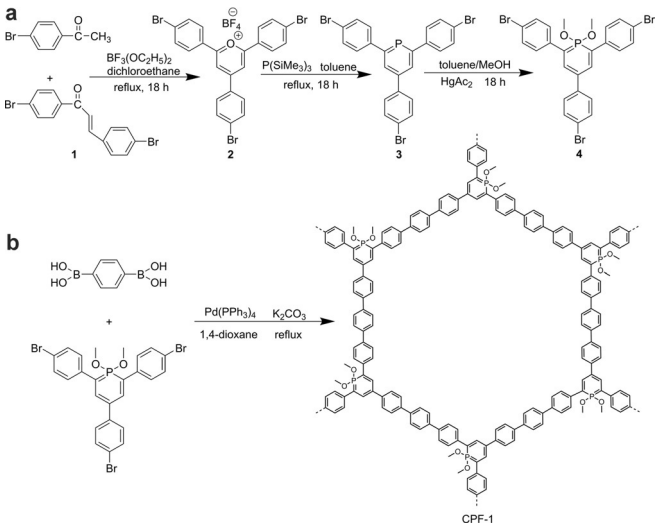

Figure 1. (a) Synthetic route for the phosphinine-based tectons **3** and **4**. (b) Suzuki–Miyaura coupling polymerization route of tecton **4** to covalent phosphinine-based framework, CPF-1.

Table S1 and discussed in more detail in the Supporting Information (Section S3).

According to Tables S1 and S2 (in the Supporting Information), the phosphinine ring is attacked and decomposes under most classical polymerization conditions. Especially for the λ^3-phosphinine compound, we were unable to find a compatible polymerization protocol. After the λ^3-phosphinine is protected by MeO- groups, the λ^5-phosphinine compound is stable in the presence of $Pd(PPh_3)_4$ and K_2CO_3, but not stable under alkaline conditions.

Even though the options for polymerization are limited, protocols such as Suzuki–Miyaura or coupling remain viable. Therefore, we chose Suzuki–Miyaura coupling in a first attempt to obtain P-containing π-conjugated frameworks, which is described above and in Figure 1 b.

Structure, composition, and morphology characterization of CPF-1

Benzene-1,4-diboronic acid, as the simplest difunctional monomer that is commercially available, was chosen for coupling with tecton **4**, aiming to form π-conjugated frameworks with a classical honeycomb-like structure. Suzuki–Miyaura coupling of tecton **4** yields a brown powder, which is insoluble in all solvents tested. We synthesized a corresponding molecular phosphinine compound, 1,1-dimethoxy-2,4,6-tri(4-biphenylyl)-λ^5-phosphinine (PMC), by Suzuki–Miyaura coupling between monomer **4** and phenylboronic acid (Figure S20 in the Supporting Information) for comparison. The structure of PMC after purification was confirmed by mass spectrometry, ^{1}H NMR and ^{31}P NMR spectroscopy (Figures S21, S22 in the Supporting Information and Figure 2 c). In the ^{31}P NMR spectrum of PMC, the signal at $\delta = 68.22$ ppm is characteristic for λ^5-phosphinine.[28b]

^{31}P magic angle spinning (MAS) solid-state NMR (ssNMR) and ^{13}C cross polarization magic angle spinning (CP-MAS) ssNMR spectra of CPF-1 are shown in Figure 2 a and b. The two peaks at $\delta = 62.30$ and 20.30 ppm in the ^{31}P MAS ssNMR spectrum of CPF-1 are assigned to the ring-P of the λ^5-phosphinine moiety and to Ph_3PO, respectively. Residues of Ph_3PO are a side product of the decomposition of the $Pd(PPh_3)_4$ catalyst (see discussion in Section S4, Figures S23, S24, Section S5, Table S4, and Figure S26 in the Supporting Information).

The ^{13}C NMR spectrum of PMC has characteristic signals at 115.82 ppm (*para*-C of P), 94.14/93.24 (*ortho*-C of P), and 51.85 ppm (C in MeO).[35] The other peaks are assigned to phenyl carbons next to the signals of [D_6]benzene (127–128 ppm). The peaks at 119.17 and 117.84 ppm in the ^{13}C NMR spectrum of monomer **4** (Figure S25 in the Supporting Information), which are assigned to halogenated aromatic carbons (C-Br), cannot be observed in spectrum of PMC nor in the spectrum of CPF-1, also corroborating the high yield of the Suzuki–Miyaura coupling reaction.

The ^{13}C CP-MAS ssNMR spectrum of CPF-1 and its assignment are shown in Figure 2 b. By comparison with the ^{13}C NMR spectra of PMC and monomer **4**, it is found that the characteristic peaks for λ^5-phosphinine are at 121.80, 88.87, 86.34, and

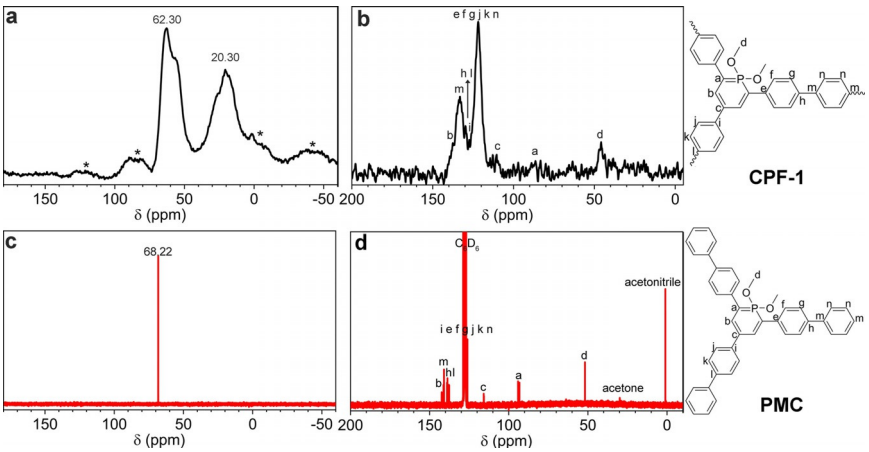

Figure 2. (a) ^{31}P magic angle spinning (MAS) solid-state NMR (ssNMR) spectrum of CPF-1. (b) ^{13}C CP-MAS ssNMR spectrum of CPF-1. (c) ^{31}P NMR spectrum of PMC in [D_6]benzene. (d) ^{13}C NMR spectrum of PMC in [D_6]benzene.

45.87 ppm, whereas the signal of the halogenated aromatic carbon (C-Br) cannot be detected.

The combustion elemental analysis (EA) and inductively coupled plasma–optical emission spectrometry (ICP-OES) results reveal that the contents of Pd (0.19 wt%), Br (1.32 wt%), and B (0.01 wt%) are quite low in CPF-1, and the mass ratio of P/H = 1.176 matches with the calculated ratio of 1.178 accurately (Section S5 and Table S3 in the Supporting Information). Further, the ICP-OES results show a mass ratio of C/P in the as-prepared polymer sample of 12.96, which is close to the theoretical value of 13.20 for perfect CPF-1. The low content of Pd, Br, and B in particular suggests that only a few unreacted end-groups remain after the polymerization and purification steps, and that the observed residuals are trapped within the polymer matrix rather than regularly built into the framework. The FTIR spectra of monomer **4**, PMC, and CPF-1 are shown in Figure 3a. The bands ranging from 2930 to 2830 cm^{-1} are assigned to C–H stretching vibrations of MeO,[36] and the bands between 1005 and 1015 cm^{-1} are assigned to C–O/P–O stretching vibrations of the λ^5-phosphinine (P-O-C).[37] These absorption bands appear in all FTIR spectra, including the λ^5-phosphinine-containing CPF-1 structure.

The powder X-ray diffraction (PXRD) patterns of CPF-1 in Figure 3b shows only a glassy polymer profile; this result is consistent with previous reports of amorphous polymer networks polymerized by Suzuki–Miyaura coupling.[38] Transmission electron microscopy (TEM) images and corresponding selected area diffraction (SAED) patterns (Figure 3d and Figure 4e) corroborate the presence of amorphous, "cauliflower"-like aggregates with sizes ranging from 0.7 to 1.5 μm with no discernible internal structure, which says two things: (1) the "cauliflower"-like aggregates of CPF-1 are indicative for point-nucleation growth, and (2) residual inorganics are dispersed in atomic (rather than macroscopic) aggregates throughout the polymer network.[9,31] SEM analysis (Figure 3c) shows globular aggregates indicative of a nucleation growth polymerisation process. Additionally, the energy-dispersive X-ray (EDX) results (Figure S27 and Table S5 in the Supporting Information) match with the composition data obtained by EA/ICP-OES.

A nitrogen sorption isotherm obtained at 77 K for CPF-1 is shown in Figure S28a (in the Supporting Information), revealing only weak porosity by Brunauer–Emmett–Teller (BET) analysis with a surface area of 72.4 $m^2 g^{-1}$. The surface area of CPF-1 is comparable to structurally analogous, carbon-only conjugated microporous polymers (CMPs).[38] Non-linear (NL)-DFT pore size distribution analysis shows pore sizes predominantly ranging between 2 and 9 nm (Figure S28b in the Supporting Information). These pores are also evident by analysis of the small-angle X-ray scattering (SAXS) data patterns (Figure S29 in the Supporting Information). This data suggests that there are some pores with average radii of 3.156 nm, ranging from 1 to 5 nm—much smaller than any of the particles observed in the SEM surveys. Compared with the BET pore size distribution results, the SAXS confirms the presence of micropores. Thermogravimetric analysis (TGA) data shows that CPF-1 is stable up to 350 °C under air and up to 700 °C under nitrogen; in fact, under non-oxidative conditions up to 67% of the mass is re-

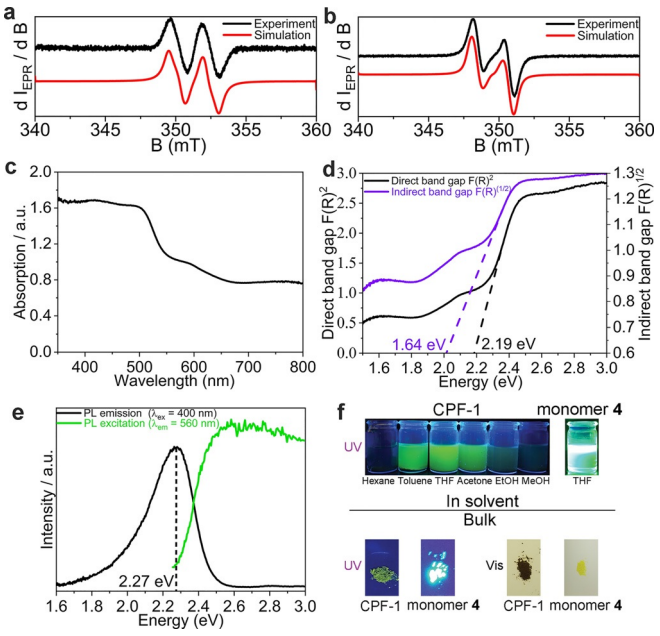

Figure 4. EPR spectra of the polycrystalline (powder) samples of (a) monomer **4** and (b) CPF-1 together with simulations of their corresponding radical cations. (c, d) Solid-state UV/Vis diffuse reflectance spectrum of CPF-1. (e) Solid-state photoluminescence emission spectrum (λ_{exc} = 400 nm) and solid-state photoluminescence excitation spectrum (λ_{em} = 560 nm) of CPF-1. (f) Images of CPF-1 dispersed in various solvents and monomer **4** illuminated with UV and visible light.

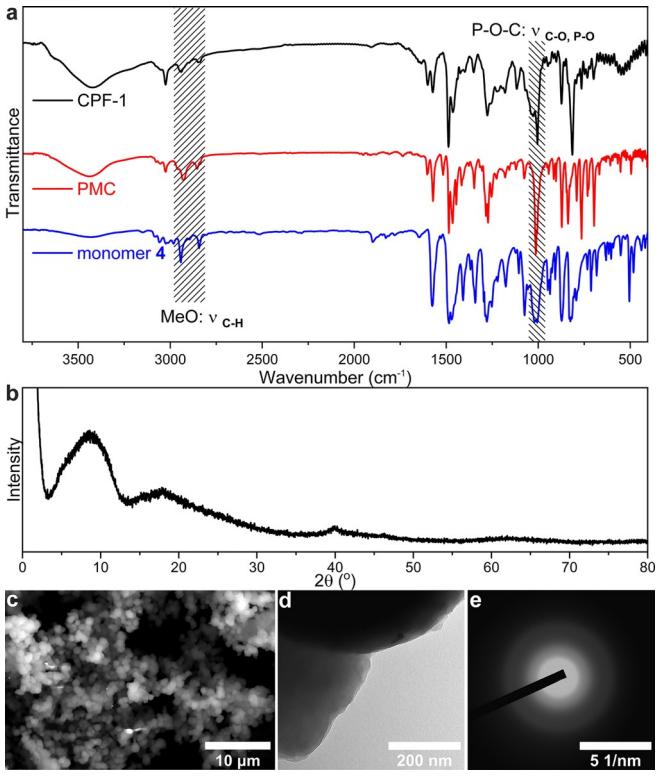

Figure 3. (a) FTIR spectra of monomer **4**, PMC, and CPF-1. (b) PXRD pattern of CPF-1. Electron microscopic investigation of CPF-1: (c) SEM image; (d) TEM image; (e) SAED image.

tained even at 1000 °C (Figure S30 in the Supporting Information). This is an extraordinarily high thermal and oxidative stability, outperforming any of the S- and N-containing polymer frameworks.[9–10]

The comprehensive structure characterization of CPF-1, as well as monomer **4** and PMC, demonstrates that a π-conjugated and stable phosphinine-based framework was successfully prepared, although some catalyst residues remain trapped in the pore structure.

Electronic and optical properties of CPF-1

We find that although CPF-1 is π-conjugated, it is not very conductive in macroscopic, pressed-pellet form with conductivity values of 1.16×10^{-12} S cm^{-1} (see Section S6 in the Supporting Information). Hence, any new, electronic effects will be found on a local, microscopic level. We see from ^{13}C CP-MAS ssNMR spectroscopy that CPF-1 has a relatively low signal-to-noise ratio even at increased MAS rates up to a maximum of 20 kHz, long contact times ($\tau = 10$ ms) and acquisition times (34.4 ms). λ^5-Phosphinine can lose an electron and be oxidized to a radical cation at a lower oxidation potential than the λ^3-phosphinine.[39] We probed this by electron paramagnetic resonance (EPR) spectroscopy of monomer **4** and CPF-1. Relevant DFT computations and simulations of EPR spectra for the λ^5-phosphinine radical cation are discussed in Section S6 (in the Supporting Information). EPR spectra of paramagnetic monomer **4** and polymer CPF-1 are shown in Figure 4a and b, together with the simulations of their corresponding radical cations. Both spectra display rhombic symmetry (simulation parameters are summarized in Table S6 in the Supporting Information) showing that radical cationic centers within the polymer as well as within the monomer do not possess a well-defined symmetry of paramagnetic centers. DFT calculation results indicate that maximum electron density is indeed situated on the P atom ring (see Tables S6 and S7 for hyperfine coupling constants and Table S8 for spin population, in the Supporting Information). Taking into account the DFT calculations, simulation of the EPR spectra, and DFT computed natural bond orbital (NBO) spin population analysis (Section S6 and Table S8 in the Supporting Information), the EPR spectra confirm that the highest spin density is localized on the central phosphinine moiety for both the tecton **4** and CPF-1. The results match some reports that state that there are radicals localized on the central λ^5-phosphinine moiety.[39–40] The radicals remain localized on the ring-phosphorus even after formation of the CPF-1 network, leading to relatively broad ssNMR signals with low signal-to-noise ratio. Furthermore, EPR results show that the Suzuki–Miyaura coupling reaction does not change the environment of the λ^5-phosphinine moieties.

According to diffuse reflectance UV/Vis spectroscopy, CPF-1 has a discernible absorption edge at around 620 nm (Figure 4c). According to the Kubelka–Munk function, this equates to a direct optical band gap of 2.19 eV and an indirect optical band gap of 1.64 eV (Figure 4d). Photoluminescence (PL) spectroscopy of CPF-1 shows one prominent peak observed at an excitation transition energy of 2.27 eV, corresponding to a wavelength of 546 nm and green fluorescence (Figure 4e). Figure 4f shows the color of CPF-1 and tecton **4** under visible light and under UV light ($\lambda_{exc} = 365$ nm). Because of the electronic interactions between conjugated polymer chains, the fluorescence efficiency of CPF-1 decreases dramatically.[38] When CPF-1 is dispersed in organic solvents, especially in THF, it again shows green fluorescence under UV light illumination ($\lambda_{exc} = 365$ nm), whereas monomer **4** shows extraordinarily intense green fluorescence.[28a]

Under 365 nm UV light illumination, the absolute measured quantum yield (QY) of monomer **4** is 43.2% (at 78.8% absorption) in the solid-state (ss). CPF-1 only has a QY in the solid state of less than 0.01% (at 81.9% absorption). Dispersed in THF, CPF-1 reveals a QY of 19.0% (at 54.3% absorption), whereas the QY of tecton **4** is 81.9% (at 28.2% absorption; Figure S33 in the Supporting Information). Hence, the fluorescence of CPF-1 is a consequence of the incorporation of the λ^5-phosphinine moiety into the polymer backbone. This fluorescence is diminished in the solid state by π–π stacking induced quenching, as observed in other π-conjugated, layered polymer systems.[28a,41]

Finally, we tried to utilize CPF-1 for some common catalytic applications such as aerobic oxidation of benzyl alcohol and photocatalytic hydrogen evolution. For aerobic oxidation experiments, we found that CPF-1 is unable to activate the aerobic oxidation of benzyl alcohol in acetonitrile at 80 °C even after 120 h (Section S7 in the Supporting Information). Similarly, photocatalytic hydrogen evolution under visible light (wavelength 380–780 nm) with triethanolamine as the sacrificial agent and 3 wt% of Pt co-catalyst yields hydrogen evolution rates lower than 1 μmol h^{-1} g^{-1}, below the detection limit. Hydrogen evolution under UV and visible light (300–2500 nm) is shown in Figure S34 (in the Supporting Information). Here, the hydrogen evolution rate of 29.3 μmol h^{-1} g^{-1} is reached when using 3 wt% of Pt co-catalyst. Hydrogen evolution rates stayed roughly constant at 33.3 μmol h^{-1} g^{-1} when no Pt co-catalyst was added. We assume that residual palladium from the network-forming reaction (0.19 wt% by ICP-OES; Table S3 in the Supporting Information) acts as a co-catalyst in this case.

Conclusion

We have synthesized an extended, π-conjugated, covalent phosphinine-based framework (CPF-1), and we addressed two gaps in research: (1) since phosphinine was first synthesized in 1966, we have achieved for the first time a successful incorporation of the six-membered phosphinine ring into a polymer by using the Suzuki–Miyaura protocol; (2) we have successfully expanded the family of potential nonmetal-containing tectons available for the rational design of π-conjugated frameworks to C, N, O, S, and now P. Two new Br-functionalized monomers containing λ^3-phosphinine and λ^5-phosphinine were obtained in the process and evaluated as building blocks in conventional polymerization protocols. Suzuki–Miyaura coupling was chosen as a conservative polymerization route with no side reactions occurring on the central P atom of the λ^5-phosphinine tecton.

We found CPF-1 not only shows remarkable thermal stability (under inert atmosphere) but also retains the green fluorescence of its phosphinine building blocks, guiding towards potential application of CPF-1 for OLEDs. As this is a first step in the investigation of the phosphinine-based polymers, it becomes clear that highly efficient catalysis and potential electronic applications will require a reliable preparation protocol of λ^3-phosphinine-based polymers in the future.[42]

Experimental Section

Synthesis of phosphinine-based precursors

The synthesis of the precursor materials 1,3-bis(4-bromophenyl)-prop-2-en-1-one (**1**) and 2,4,6-tri(4-bromophenyl)pyrylium tetrafluoroborate (**2**) is given in the Supporting Information (Section S1).

Synthesis of 2,4,6-tri(4-bromophenyl)-λ^3-phosphinine (3)

The preparation procedure is a modified method based on previous reports for phosphinine compounds.[28b,32] Compound **2** (5.21 g, 8.20 mmol) and anhydrous toluene (40 mL) were added to a 100 mL one-neck flask under inert atmosphere in a glovebox. $P(SiMe_3)_3$ (2.06 g, 8.20 mmol) was added dropwise to the flask under continuous stirring. The flask was connected to argon atmosphere via a Schlenk line, and the mixture was stirred and heated at reflux for 18 h. After volatiles were removed under vacuum, the residue was purified by column chromatography on silica gel (eluent hexane/CH_2Cl_2 = 9:1) to give 3.10 g (5.52 mmol for $C_{23}H_{14}Br_3P$, 67.3% yield) of 2,4,6-tri(4-bromophenyl)-λ^3-phosphinine (**3**) as a white solid. ^{1}H NMR (400 MHz, $(CD_3)_2CO$): δ = 8.63 (2H, d, J = 6.0 Hz), 7.91–7.86 (2H, m), 7.85–7.78 (4H, m), 7.78–7.70 ppm (6H, m) (see Figure S4 in the Supporting Information); ^{31}P NMR (162 MHz, $(CD_3)_2CO$): δ = 186.27 ppm (see Figure S5 in the Supporting Information). Note: 2,4,6-tri(4-bromophenyl)-λ^3-phosphinine is not stable in $CDCl_3$.

Synthesis of 1,1-dimethoxy-2,4,6-tri(4-bromophenyl)-λ^5-phosphinine (4)

The preparation procedure was adapted from Dimruth et al.[43] Compound **3** (3.10 g, 5.52 mmol), mercury(II) acetate (1.76 g, 5.53 mmol), anhydrous MeOH (150 mL) and anhydrous toluene (150 mL) were stirred under argon atmosphere at room temperature for 12 h. After the liquid was removed under vacuum, the residue was purified by column chromatography on silica gel (eluent hexane/CH_2Cl_2 = 8:2) to give 2.40 g (3.85 mmol) crude product. The crude product was recrystallized from acetonitrile overnight to form the green/yellow product 1,1-dimethoxy-2,4,6-tri(4-bromophenyl)-λ^5-phosphinine (**4**, 2.06 g, 3.31 mmol for $C_{25}H_{20}Br_3O_2P$, 60.0% yield). ^{1}H NMR (400 MHz, $(CD_3)_2CO$): δ = 8.00 (2H, d, J = 36.6 Hz), 7.64–7.57 (8H, m), 7.57–7.44 (4H, m), 3.50 ppm (6H, d, J = 13.8 Hz) (see Figure S6 in the Supporting Information); ^{31}P NMR (162 MHz, $(CD_3)_2CO$): δ = 66.44 ppm (see Figure S7); MS (APCI): calcd for $[C_{25}H_{21}O_2Br_3P]$: 620.88238; found: 620.88248 (see Figure S8 in the Supporting Information).

Synthesis of π-conjugated covalent phosphinine-based framework (CPF-1)

Polymerization was achieved with a palladium-catalyzed Suzuki–Miyaura coupling process.[34c,38,44] Monomer **4** (732 mg, 1.17 mmol), benzene-1,4-diboronic acid (292 mg, 1.76 mmol), and $Pd(PPh_3)_4$ catalyst (102 mg, 0.0880 mmol) were added to a 250 mL three-neck flask and purged under argon. 1,4-Dioxane (80 mL) was degassed by argon bubbling for 20 min and then added to the flask under continuous stirring. Aqueous K_2CO_3 solution (12.5 mL) was degassed by argon bubbling for 20 min and then added to the flask. The mixture was degassed by argon bubbling for a further 30 min, and subsequently stirred and heated at reflux under argon atmosphere for 80 h. The precipitate was collected by filtration and washed with THF, $CHCl_3$, hot water, and MeOH, and further purification was carried out by Soxhlet extraction for 2 days by using THF and MeOH. The product was washed with water (200 mL) at 90 °C three times to remove K_2CO_3, and the brown powder was finally dried at 120 °C for 12 h under vacuum to afford CPF-1 (0.4558 g, 0.458 mmol for $C_{68}H_{52}O_4P_2$, 78.3% yield). Elemental analysis calcd (%) for CPF-1: C 82.07, H 5.28, O 6.43, P 6.22; found: C 73.47, H 4.82, P 5.67, K 0.3, Pd 0.19, Br 1.32, B 0.01.

Acknowledgments

J.H. carried out the synthetic experiments, analyzed the data, and wrote the paper. J.T. carried out the EPR measurements and analysis, EPR simulation, and DFT computation. R.K. carried out the BET measurements and analysis, and the aerobic oxidation experiments. C.W. and U.R. carried out the optical property measurements and analysis. M.D. carried out the ss-NMR measurements and NMR analysis. G.J.S. and B.R.P. carried out the SAXS-WAXS measurements and analysis. Y.T. and S.R. carried out the hydrogen evolution experiments and analysis. M.J.B conceived the project and wrote the paper. We thank Barbora Balcarova for N_2 sorption measurements, Dr. Lucie Bednárová for FTIR spectroscopy, Dr. Radek Pohl for NMR measurements, Romana Hadravová for TEM measurements, Stanislava Matějková for EA/ICP-OES, Dr. Yu Noda for conductivity measurements, Yi Xiong for graphical abstract design, Pengbo Lyu and Prof. Dr. Petr Nachtigall for of DFT calculated EPR parameters. M.J.B. thanks the European Research Council (ERC) for funding under the Starting Grant Scheme (BEGMAT-678462).

Conflict of interest

The authors declare no conflict of interest.

Keywords: fluorescence · phosphinine · polymers · Suzuki–Miyaura coupling · π-conjugated frameworks

[1] X. Zou, H. Ren, G. Zhu, *Chem. Commun.* **2013**, *49*, 3925 – 3936.
[2] R. Dawson, A. Trewin, in *Porous Polymers: Design, Synthesis and Application* (Eds.: S. Qiu, T. Ben), Royal Society of Chemistry, Cambridge, **2015**, Ch. 7, pp. 155 – 185.
[3] T. Ben, S. Qiu, *CrystEngComm* **2013**, *15*, 17 – 26.
[4] W. Lu, D. Yuan, D. Zhao, C. I. Schilling, O. Plietzsch, T. Muller, S. Bräse, J. Guenther, J. Blümel, R. Krishna, *Chem. Mater.* **2010**, *22*, 5964 – 5972.
[5] J. X. Jiang, F. Su, A. Trewin, C. D. Wood, N. L. Campbell, H. Niu, C. Dickinson, A. Y. Ganin, M. J. Rosseinsky, Y. Z. Khimyak, *Angew. Chem. Int. Ed.* **2007**, *46*, 8574 – 8578; *Angew. Chem.* **2007**, *119*, 8728 – 8732.
[6] X. Liu, Y. Xu, D. Jiang, *J. Am. Chem. Soc.* **2012**, *134*, 8738 – 8741.
[7] Y. Xu, S. Jin, H. Xu, A. Nagai, D. Jiang, *Chem. Soc. Rev.* **2013**, *42*, 8012 – 8031.

[8] G. Algara-Siller, N. Severin, S. Y. Chong, T. Björkman, R. G. Palgrave, A. Laybourn, M. Antonietti, Y. Z. Khimyak, A. V. Krasheninnikov, J. P. Rabe, *Angew. Chem. Int. Ed.* **2014**, *53*, 7450 – 7455; *Angew. Chem.* **2014**, *126*, 7580 – 7585.

[9] a) P. Katekomol, J. R. M. Roeser, M. Bojdys, J. Weber, A. Thomas, *Chem. Mater.* **2013**, *25*, 1542 – 1548; b) S. Ren, M. J. Bojdys, R. Dawson, A. Laybourn, Y. Z. Khimyak, D. J. Adams, A. I. Cooper, *Adv. Mater.* **2012**, *24*, 2357 – 2361; c) M. J. Bojdys, J. Jeromenok, A. Thomas, M. Antonietti, *Adv. Mater.* **2010**, *22*, 2202 – 2205.

[10] a) D. Schwarz, A. Acharja, A. Ichangi, P. Lyu, M. V. Opanasenko, F. R. Goßler, T. A. König, J. Čejka, P. Nachtigall, A. Thomas, *Chem. Eur. J.* **2018**, *24*, 11916 – 11921; b) D. Schwarz, Y. S. Kochergin, A. Acharjya, A. Ichangi, M. V. Opanasenko, J. Čejka, U. Lappan, P. Arki, J. He, J. Schmidt, *Chem. Eur. J.* **2017**, *23*, 13023 – 13027.

[11] J. Roeser, D. Prill, M. J. Bojdys, P. Fayon, A. Trewin, A. N. Fitch, M. U. Schmidt, A. Thomas, *Nat. Chem.* **2017**, *9*, 977 – 982.

[12] R. Palkovits, M. Antonietti, P. Kuhn, A. Thomas, F. Schüth, *Angew. Chem. Int. Ed.* **2009**, *48*, 6909 – 6912; *Angew. Chem.* **2009**, *121*, 7042 – 7045.

[13] Y. S. Kochergin, D. Schwarz, A. Acharjya, A. Ichangi, R. Kulkarni, P. Eliášová, J. Vacek, J. Schmidt, A. Thomas, M. J. Bojdys, *Angew. Chem. Int. Ed.* **2018**, *57*, 14188 – 14192; *Angew. Chem.* **2018**, *130*, 14384 – 14388.

[14] A. I. Cooper, *Adv. Mater.* **2009**, *21*, 1291 – 1295.

[15] a) A. Thomas, *Angew. Chem. Int. Ed.* **2010**, *49*, 8328 – 8344; *Angew. Chem.* **2010**, *122*, 8506 – 8523; b) Y. Xu, Z. Lin, X. Huang, Y. Wang, Y. Huang, X. Duan, *Adv. Mater.* **2013**, *25*, 5779 – 5784.

[16] W. Lu, D. Yuan, J. Sculley, D. Zhao, R. Krishna, H.-C. Zhou, *J. Am. Chem. Soc.* **2011**, *133*, 18126 – 18129.

[17] M. J. Bojdys, *Macromol. Chem. Phys.* **2016**, *217*, 232 – 241.

[18] a) S. B. Alahakoon, C. M. Thompson, G. Occhialini, R. A. Smaldone, *ChemSusChem* **2017**, *10*, 2116 – 2129; b) N. Huang, P. Wang, D. Jiang, *Nat. Rev. Mater.* **2016**, *1*, 16068; c) U. Díaz, A. Corma, *Coord. Chem. Rev.* **2016**, *311*, 85 – 124.

[19] a) K. Abersfelder, A. J. White, H. S. Rzepa, D. Scheschkewitz, *Science* **2010**, *327*, 564 – 566; b) P. Le Floch, in *Phosphorous Heterocycles I*, Springer, Berlin, **2008**, pp. 147 – 184.

[20] a) S. Zhang, X. Zhao, B. Li, C. Bai, Y. Li, L. Wang, R. Wen, M. Zhang, L. Ma, S. Li, *J. Hazard. Mater.* **2016**, *314*, 95 – 104; b) M. A. Patel, F. Luo, M. R. Khoshi, E. Rabie, Q. Zhang, C. R. Flach, R. Mendelsohn, E. Garfunkel, M. Szostak, H. He, *ACS Nano* **2016**, *10*, 2305 – 2315.

[21] B. W. Rawe, D. P. Gates, *Angew. Chem. Int. Ed.* **2015**, *54*, 11438 – 11442; *Angew. Chem.* **2015**, *127*, 11600 – 11604.

[22] R.-J. Jeng, S.-M. Shau, J.-J. Lin, W.-C. Su, Y.-S. Chiu, *Eur. Polym. J.* **2002**, *38*, 683 – 693.

[23] a) P. Le Floch, *Coord. Chem. Rev.* **2006**, *250*, 627 – 681; b) X. D. Jiang, J. Zhao, D. Xi, H. Yu, J. Guan, S. Li, C. L. Sun, L. J. Xiao, *Chem. Eur. J.* **2015**, *21*, 6079 – 6082.

[24] a) P. Mohanty, L. D. Kull, K. Landskron, *Nat. Commun.* **2011**, *2*, 401; b) Z. Hu, Z. Shen, C. Y. Jimmy, *Green Chem.* **2017**, *19*, 588 – 613; c) L. Xu, R. Hu, B. Z. Tang, *Macromolecules* **2017**, *50*, 6043 – 6053; d) S. Popa, S. Iliescu, G. Ilia, N. Plesu, A. Popa, A. Visa, L. Macarie, *Eur. Polym. J.* **2017**, *94*, 286 – 298.

[25] a) P. Le Floch, in *Phosphorus – Carbon Heterocyclic Chemistry*, Elsevier, Amsterdam, **2001**, pp. 485 – 533; b) C. S. Lin, J. Li, C. W. Liu, *Chin. J. Chem.* **1997**, *15*, 289 – 295.

[26] a) H. Zhang, X. Li, D. Zhang, L. Zhang, M. Kapilashrami, T. Sun, P.-A. Glans, J. Zhu, J. Zhong, Z. Hu, *Carbon* **2016**, *103*, 480 – 487; b) Y. Zhou, L. Zhang, J. Liu, X. Fan, B. Wang, M. Wang, W. Ren, J. Wang, M. Li, J. Shi, *J. Mater. Chem. A* **2015**, *3*, 3862 – 3867; c) L. Jing, R. Zhu, D. L. Phillips, J. C. Yu, *Adv. Funct. Mater.* **2017**, *27*, 1703484; d) J. Ran, T. Y. Ma, G. Gao, X.-W. Du, S. Z. Qiao, *Energy Environ. Sci.* **2015**, *8*, 3708 – 3717; e) S. Guo, Z. Deng, M. Li, B. Jiang, C. Tian, Q. Pan, H. Fu, *Angew. Chem. Int. Ed.* **2016**, *55*, 1830 – 1834; *Angew. Chem.* **2016**, *128*, 1862 – 1866; f) Y.-P. Zhu, T.-Z. Ren, Z.-Y. Yuan, *ACS Appl. Mater. Interfaces* **2015**, *7*, 16850 – 16856; g) Y. Zhang, T. Mori, J. Ye, M. Antonietti, *J. Am. Chem. Soc.* **2010**, *132*, 6294 – 6295.

[27] G. Märkl, *Angew. Chem. Int. Ed. Engl.* **1966**, *5*, 846 – 847; *Angew. Chem.* **1966**, *78*, 907 – 908.

[28] a) N. Hashimoto, R. Umano, Y. Ochi, K. Shimahara, J. Nakamura, S. Mori, H. Ohta, Y. Watanabe, M. Hayashi, *J. Am. Chem. Soc.* **2018**, *140*, 2046 – 2049; b) C. Müller, D. Wasserberg, J. J. Weemers, E. A. Pidko, S. Hoffmann, M. Lutz, A. L. Spek, S. C. Meskers, R. A. Janssen, R. A. van Santen, *Chem. Eur. J.* **2007**, *13*, 4548 – 4559.

[29] a) C. Müller, D. Vogt, *Comptes Rendus Chimie* **2010**, *13*, 1127 – 1143; b) H. Trauner, P. Le Floch, J.-M. Lefour, L. Ricard, F. Mathey, *Synthesis* **1995**, *1995*, 717 – 726; c) P. Le Floch, D. Carmichael, L. Ricard, F. Mathey, *J. Am. Chem. Soc.* **1993**, *115*, 10665 – 10670.

[30] P. Tokarz, P. M. Zagórski, *Chem. Heterocycl. Compd.* **2017**, *53*, 858 – 860.

[31] P. Kuhn, A. Forget, J. Hartmann, A. Thomas, M. Antonietti, *Adv. Mater.* **2009**, *21*, 897 – 901.

[32] L. E. Broeckx, S. Güven, F. J. Heutz, M. Lutz, D. Vogt, C. Müller, *Chem. Eur. J.* **2013**, *19*, 13087 – 13098.

[33] J. Hassan, M. Sevignon, C. Gozzi, E. Schulz, M. Lemaire, *Chem. Rev.* **2002**, *102*, 1359 – 1470.

[34] a) D. Schwarz, Y. S. Kochergin, A. Acharja, A. Ichangi, M. V. Opanasenko, J. Čejka, U. Lappan, P. Arki, J. He, J. Schmidt, *Chem. Eur. J.* **2017**, *23*, 13023 – 13027; b) T. D. Nelson, R. D. Crouch, *Org. React.* **2004**, *63*, 265 – 555; c) M. Alvaro, C. Aprile, B. Ferrer, H. Garcia, *J. Am. Chem. Soc.* **2007**, *129*, 5647 – 5655; d) M.-S. Kim, C. S. Phang, Y. K. Jeong, J. K. Park, *Polym. Chem.* **2017**, *8*, 5655 – 5659; e) D. Schwarz, Y. Noda, J. Klouda, K. Schwarzová-Pecková, J. Tarábek, J. Rybáček, J. Janoušek, F. Simon, M. V. Opanasenko, J. Čejka, *Adv. Mater.* **2017**, *29*, 1703399.

[35] H. Kanter, W. Mach, K. Dimroth, *Eur. J. Inorg. Chem.* **1977**, *110*, 395 – 422.

[36] J. Coates, in *Encyclopedia of Analytical Chemistry*, Wiley, Hoboken, **2000**.

[37] K. Dimroth, M. Lückoff, *Eur. J. Inorg. Chem.* **1980**, *113*, 3313 – 3317.

[38] R. S. Sprick, B. Bonillo, M. Sachs, R. Clowes, J. R. Durrant, D. J. Adams, A. I. Cooper, *Chem. Commun.* **2016**, *52*, 10008 – 10011.

[39] K. Dimroth, *Phosphorus – Carbon Double Bonds*, Springer, Berlin **1973**, pp. 1 – 147.

[40] K. Dimroth, W. Heide, *Chem. Ber.* **1981**, *114*, 3004 – 3018.

[41] Z. Hu, A. P. Willard, R. J. Ono, C. W. Bielawski, P. J. Rossky, D. A. V. Bout, *Nat. Commun.* **2015**, *6*, 8246.

[42] C. Yang, B. C. Ma, L. Zhang, S. Lin, S. Ghasimi, K. Landfester, K. A. Zhang, X. Wang, *Angew. Chem. Int. Ed.* **2016**, *55*, 9202 – 9206; *Angew. Chem.* **2016**, *128*, 9348 – 9352.

[43] K. Dimroth, W. Städe, *Angew. Chem. Int. Ed. Engl.* **1968**, *7*, 881 – 882; *Angew. Chem.* **1968**, *80*, 966 – 967.

[44] A. Suzuki, *Angew. Chem. Int. Ed.* **2011**, *50*, 6722 – 6737; *Angew. Chem.* **2011**, *123*, 6854 – 6869.

Manuscript received: January 18, 2019

Accepted manuscript online: July 19, 2019

Version of record online: August 13, 2019

